

- J.M., Marvin, D.A. and Perham, R.N., *J. Mol. Biol.* (1998) 283, 155-177.
- [29] Yamashita, I., Hasegawa, K., Suzuki, H., Vonderviszt, F., Mimori-Kiyosue, Y. and Namba, K., *Nature Struct. Biol.* (1998) 5, 125-132.
- [30] Yamashita, I., Suzuki, H. and Namba, K., *J. Mol. Biol.* (1998) 278, 609-615.
- [31] Erickson, J.W. and Bancroft, J.B., *Virology* (1978) 90, 36-46.
- [32] Goodman, R., *Virology* (1975) 68, 287-298.

Crystallisation in block copolymer melts: soft-hard templating

J.Patrick. A. Fairclough¹, Shao-Min. Mai², Mark W. Matsen³, Wim Bras⁴, Loic Messe¹, Simon Turner¹, Anthony Gleeson⁵, Colin Booth², Ian W. Hamley⁶ and Anthony J. Ryan¹

[1].Dept of Chemistry, University of Sheffield, Sheffield S3 7HF, UK.

[2].Dept of Chemistry, University of Manchester, Manchester M13 9PL, UK

[3].Polymer Science Centre, University of Reading, Reading RG6 6AF, UK.

[4].Netherlands Organisation for Scientific Research, DUBBLE CRG, ESRF, F38043, Grenoble Cedex, France.

[5].CLRC Daresbury Laboratory, Warrington, WA4 4AD, UK.

[6].School of Chemistry, University of Leeds, Leeds LS2 9JT, UK.

The crystallisation of shear oriented oxyethylene/oxybutylene (E/B) diblock copolymers has been studied by simultaneous SAXS and WAXS. Crystallisation of ordered melts can be accompanied by a change in length scale and retention of the melt orientation. Lamellar melts crystallise with an increase in length scale with multiply-folded E blocks and the B blocks slightly stretched from their melt conformation. Crystallisation from oriented gyroid melts leads to an increase in length scale with preferred melt directions being selected. The retention of layer planes on crystallisation from an ordered melt is caused by the local stretching of chains and the locally one dimensional structure, despite the relative strengths of the structural process. We demonstrate that an interfacial preordering effect can cause crystallographic register to jump length scales in a soft matter system showing epitaxial crystallisation.

Introduction

Self-assembly of amphiphilic molecules provides one of the fundamental structure directing processes for building hierarchical structures in nature¹. The universality of pattern formation by lipid membranes, lyotropic and thermotropic liquid crystals, and block copolymers¹⁻³, all soft-structures

that are closely related to biological materials, is striking. Classical structures of lamellae, hexagonally ordered cylinders and cubic arrays of spheres are well established^{1,4} and it is easy to visualise how they act as templates. Complex cubic structures, such as the bicontinuous double diamond (Pn3m) and gyroid (Ia3d) have been found in lyotropic liquid crystals² and in block copolymer melts⁵⁻⁷ and solutions⁸ as well as in naturally occurring lipids^{1,9,10}. These also act as templates but in a more subtle manner. Here we report a transformation from a soft structure (block copolymer melt) to a hard structure (semi-crystalline block copolymer) with conservation of preferred lattice directions and a doubling of the lattice spacing.

How can one make a large hierarchical structure? Hard (crystalline) materials cannot form large scale structures directly but need soft materials, which have the ability to self-assemble, to act as templates and direct structure formation. Another important question is, what circumstances allow the retention of crystallographic register, especially when the free energy changes associated with the two processes, templating and hard material growth are quite different? Structures in lipids, liquid crystals and block copolymers are typical of "soft" condensed matter where the material has a large scale structure with crystallographic register, but where the local atomic structure is liquid-like and disordered. These large scale structures are formed due to a balance of forces minimising the Gibbs energy and are truly at dynamic equilibrium¹⁰. In the case of block copolymers the important features are the configurational entropy of the molecules and the formation of interfacial area. The theory, which describes these phenomena, is well developed¹¹ and gives accurate predictions of phase behaviour. The gyroid (Ia3d) phase has been observed between the lamellar and hexagonal packed cylinder phases in the diblock copolymer phase diagram close to the order-disorder transition^{6,12}; it comprises cylindrical channels of the minority material joined by 3-fold connectors, two such lattices with opposite chirality interpenetrate through a matrix.

One important class of structure direction is soft-soft templating between mesoscopic structures. Transformations between adjacent gyroid and lamellar or hexagonal phases have attracted attention because they are related to the structural transitions

which occur when cells fuse or rupture. A number of studies of anionic and non-ionic surfactants have provided evidence of epitaxial relationships in transformations of gyroid to lamellar^{13,14} with growth proceeding along [111] directions without change in lattice parameters. This is thought to be related to the orientation of the 3-fold connectors within the unit cell. A similar epitaxial relationship has been observed for a diblock copolymer melt¹⁵ where the lamellar phase grows from the gyroid without long-range transport of material and with preservation of orientation in some layer planes. In these epitaxial transformations the lattice spacing is either conserved or changes smoothly as the high-symmetry cubic structure transforms into the lower symmetry layered or rod-like structure. This is usual in structural transformation in both soft- and hard-condensed matter. Soft-hard templating, by block copolymers and surfactants, of porous and composite structure on the nanometer scale has provoked much interest for formation of mesostructured inorganic^{16,17} and organic materials¹⁸. In these cases there is no crystallographic register between the soft template and the growing hard phase and structural transformations are observed as chemical reactions change the thermodynamic interactions between components¹⁸. However, if epitaxy is observed, then there is nearly always a continuous change in lattice parameters.

Experimental

The amphiphilic system reported here has been extensively studied including self-assembly in dilute and concentrated aqueous solutions¹⁹, microphase separation in the melt²⁰ and crystallisation behaviour²¹. Block copolymers with narrow molecular weight distributions were prepared by sequential anionic polymerisation of ethylene oxide (E) followed by 1,2-butylene oxide (B). Vacuum line and ampoule techniques were used throughout and the copolymers were characterised by gel permeation chromatography and ¹³C NMR spectroscopy. The molecular characteristics are expressed in E_mB_n notation where the subscripts denote the average numbers of repeat units.

Simultaneous SAXS/WAXS measurements were made on beamline 16.1 at the Daresbury Synchrotron Radiation Source or on the DUBBLE beamline at the European Synchrotron Radiation Source (ESRF). At Daresbury the incident beam was 1.4 Å and a Fuji

image plate at 10 cm was used to record the WAXS pattern with a 10 mm hole to allow the SAXS pattern to develop out at 3 m for recording on an area detector. At the ESRF the incident beam was 1.0 Å and an area detector was used to record the SAXS at 4 m. The sample thickness was 1 mm and the beam passed through a hole of 3 mm which was covered with Kapton™ tape. The sample was oriented by shearing the ordered melt, for 50 cycles at approximately 1 Hz and 200% strain, in a heated cell consisting of a piece of brass with machined side grooves to allow movement of a parallel brass slider during shear. The polymer temperature was monitored by a thermocouple. Quiescent cooling after shear orientation allowed the epitaxial relationships to be observed.

Results and Discussion

The crystallisation of melts of E_mB_n copolymers has been studied in some detail²¹ and the orientation of the crystal stems perpendicular to lamellar interfaces is well established. This is soft-hard templating but with obvious epitaxial relationships. The simplest case of a copolymer with a lamellar melt phase and a lamellar semi-crystalline phase is illustrated in Figure 1a by a schematic of the molecular conformations of $E_{76}B_{38}$ in the equilibrium melt and crystallised states. In the melt the characteristic length scale, D , is that of the stretched coil with a length dependent on the radius of gyration, R_g , whereas in the crystalline state the characteristic length scale is the related to the extended chain length, L . The low temperature structure is a once-folded E block (two crystal stems) and an unfolded, stretched B block: an unfolded E chain would not be possible due to conservation of volume. The SAXS pattern in Figure 1b is obtained from a sample of $E_{76}B_{38}$ that was shear oriented prior to crystallisation. It shows first order reflections from the lamellar crystals with a d-spacing of 224 Å. There are clearly resolved 2nd, 3rd and 4th order reflections and the minimal arcing illustrates that the material is a monodomain with lamellae oriented in the shear direction. The simultaneously recorded WAXS pattern in Figure 1c confirms that the E chains are oriented perpendicular to the lamellar interfaces, the strong equatorial reflections derived from the c-axis {001} of the helical E block²². SAXS²¹ shows a change in length scale from 109 Å in the ordered melt to 224 Å in the crystal phase, i.e. there is a step change in lattice spacing on

Observed intensity	<211> Azimuthal position/ ^o	Predicted intensity
1	0,180	1
1.3	28.1,151.9,208.1,311.9	1.14
3.2	70.5,109.5,250.5,289.5	1.50

Observed intensity	<220> Azimuthal position/ ^o	Predicted intensity
3.2	0,180	1.15
1	54.7,125.3,234.7,305.3	1

Table 1: The predicted intensities from a gyroid melt randomly oriented about the [111] direction [15] compared to those observed in the azimuthal intensity measurements.

transformation from the soft ordered melt structure to the hard semicrystalline solid structure with an approximate doubling of lattice spacing due to stretching of chains perpendicular to the lamellar interface with corresponding lateral contraction.

The terms "soft" and "hard", as applied here to the ordered melt and semicrystalline solid, are justified by the enthalpy of formation of the structures and the mechanical properties of the materials. High resolution calorimetry²³ studies on $E_{60}B_{29}$ show that the latent heat of the fusion process is $90.2 \pm 2 \text{ Jg}^{-1}$ whereas that of the order-disorder transition in the melt is $0.171 \pm 0.003 \text{ J g}^{-1}$. The enthalpy of formation of crystals is 500 times larger than that of the ordered melt. Similarly the shear modulus of the semicrystalline polymer is 10^7 Pa whereas that of the ordered melt is 10^5 Pa .

Ordered block copolymer melts have chains that are stretched compared to the random (Gaussian) conformations^{3,11}. The characteristic length of a strongly segregated melt scales with $N^{2/3}$ compared with $N^{1/2}$ for a Gaussian chain. Furthermore, the stretching is not uniform, chain segments are more strongly oriented across the interface between the two chain types. It is feasible that it is the local orientation of chain segments perpendicular to the interfaces that nucleates crystallisation. The local orientation reduces the crystallisation energy barrier (crystallisation in polymers requires development of orientational order along the chain) and promotes crystal growth. For this reason the vast majority of semicrystalline block copolymers show stems

perpendicular to lamellar surfaces. The conditions for formation of other orientations and morphologies must be strongly forcing, i.e. confinement of the crystallising chains by hard walls^{24,25} and with chain imperfections that prevent formation of large crystals.

The retention of orientation of layer planes on crystallisation from a lamellar ordered melt is not unexpected given the local stretching of chains and the one dimensional structure, despite the strong driving force for the transition. What is unexpected, however, is that a more complex soft structure will also direct crystallisation processes. The SAXS patterns in Figure 2 follow the transformation of a gyroid melt into a lamellar crystal. The SAXS pattern in Figure 2a was obtained following large amplitude oscillatory shear and is typical^{5,6,12,15} of the gyroid morphology. The 10 spot pattern is from a directionally oriented Ia3d crystals with the zone axis along the [111] lattice direction which is oriented parallel to the shear direction^{15,26}. This oriented melt structure was allowed to cool from 80°C to 20°C over a period of an hour. Orientation was maintained after shearing and many higher order reflections were sampled. Once crystallisation starts strong scattering was observed inside the 211 reflections of the melt. The example shown in Figure 2b shows simultaneous growth in two of the $\langle 211 \rangle$ directions. Repeated experiments (at Daresbury and the ESRF) showed crystal growth to be observed preferentially in three of the five {211} planes. These lamellar crystals are consuming the ordered melt the presence of which is confirmed since the higher orders of Ia3d are still clearly visible. Eventually (Figure 2c) the gyroid melt is nearly all consumed and higher order reflections can be seen for the lamellar crystals. There has been a transformation in two of the [211] directions of the Ia3d cubic structure with d-spacing $123 \pm 2 \text{ \AA}$ to an oriented lamellar structure with d-spacing $237 \pm 5 \text{ \AA}$. If there is epitaxy from the Ia3d to the lamellar structure then there are 24 equivalent planes available. In this experiment we have Bragg sampled two of these planes during the crystallisation of a {111} zone oriented crystal of Ia3d melt.

In the gyroid morphology, chain stretching is uniform (within 7%)²⁶ across the interface between microphases and consequently crystallisation can nucleate anywhere around this surface. The absolute magnitude of the change in characteristic length on crystallisation is determined by the crystallisation

temperature and block lengths, in the example given here the length scale doubles. The effective doubling of the plane separation is illustrated in Figure 3 (a, b) where unit cells are shown transforming along {111} into 2 lamellar unit cells. Figure 3c shows average segmental density profiles across the [112] and [220] directions of the gyroid phase, calculated using self-consistent field methods^{4,11,26}, and the density map of the structure as it would appear in the TEM looking down the {111} axis. These calculations provide strong evidence that lamellae orient along [211] directions because that is the direction in which the gyroid phase most resembles a lamellar phase.

The stretching is localised to the interface and this is where we would expect crystallisation to initiate. Statistically crystals that initiate are likely to grow fastest in the direction most able to provide room for growth, i.e. the most lamellar-like directions. Consequently, the crystallisation follows the lamellar like direction initially and then breaks out to a longer length scale. The initial crystallisation is the symmetry breaking step and retains the preferred direction of the soft cubic structure even though the length scale increases. Recent experimental and theoretical²⁷ work on polymer crystallisation has shown that the local structure of the polymer melt, prior to crystallisation, has a strong influence on the nature of the crystallisation process. The local orientation at the block copolymer interfaces reduces the crystallisation energy barrier causing the epitaxial relationships observed.

In Figure 4 we compare the scattering pattern from the melt and the crystals to confirm the epitaxial relationships. In Figure 4a the melt and crystal structures from a small scattering volume (0.125 mm^3) clearly illustrate that crystallisation selects the $\langle 211 \rangle$ directions and the lamellar peaks lie on these planes separated by 70.5° . We suspect that there are two domains in the Bragg condition giving rise to these two sets of lamellar reflections and this gives indirect evidence of the grain size. In Figure 4b, however, there is a much larger scattering volume (2.5 mm^3) and more lamellar domains are sampled. Now three of the five [211] directions are obviously preferred and these are highlighted by the solid lines Figure 4b and by the azimuthal intensity scans in Figure 4c. In repeated crystallisation we do not observe strong crystalline reflections in the directions highlighted by the dotted lines.

The Ia3d structure obtained by large amplitude

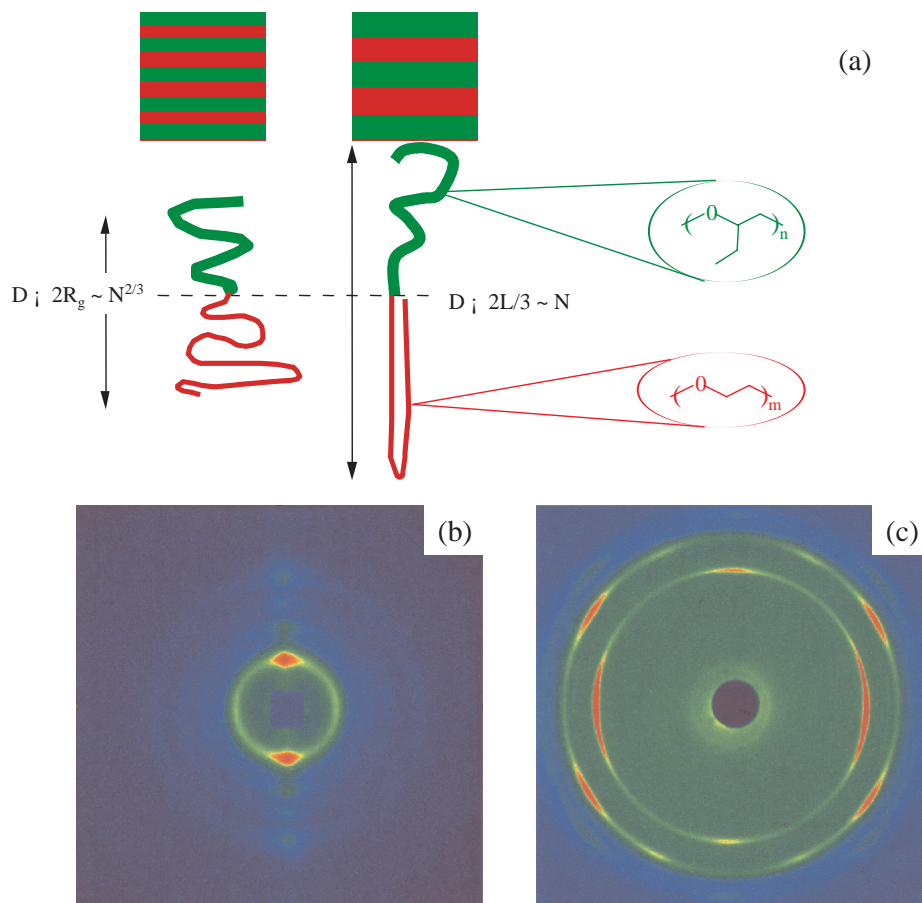


Figure 1: (a) A schematic representation of block copolymer chain conformation in the molten and crystalline states. In the disordered melt the chains are Gaussian and have a size which scales as $N^{1/2}$, whereas in the ordered melt the chains are stretched from their Gaussian conformations and have a domain spacing which scales as $N^{2/3}$. When one of the blocks crystallises into a straight stem the amorphous chains are stretched from their Gaussian conformations and have a domain spacing that scales as N . (b) Small angle X-ray scattering data from a sample of $E_{76}B_{38}$ that had been crystallised after shearing in the melt. It shows a pair of first order reflections from the lamellar crystals with a d-spacing of 224 Å. There are clearly resolved 2nd, 3rd and 4th order reflections and the minimal arcing illustrates that the material is a monodomain with lamellae oriented in the shear direction. (c) Wide angle X-ray diffraction data from a sample of $E_{76}B_{38}$ that had been crystallised after shearing in the melt. Fibre diffraction of poly(oxyethylene) [22] shows that the E chains are oriented perpendicular to the lamellar interfaces as the strong equatorial reflection is the c-axis (001 reflection) of the unit cell. Simultaneous SAXS/WAXS measurements were made on beamline 16.1 at the Daresbury Synchrotron Radiation Source using a Fuji image plate at 10 cm to record the WAXS pattern with a 10 mm hole to allow the SAXS pattern to develop out at 3 m. The sample thickness was 1 mm and the beam passed through a hole of 3 mm which was covered with Kapton™ tape. The sample was oriented by shearing the ordered melt, for 50 cycles at approximately 1 Hz and 200% strain, in a heated cell consisting of a piece of brass with machined side grooves to allow movement of a parallel brass slider during shear, the polymer temperature was monitored by a thermocouple. Quiescent cooling after shear orientation allowed the epitaxial relationships to be observed.

oscillatory shear is a highly twinned body centred cubic structure with a [111] direction along the shear direction¹⁵ The intensities predicted for the 211 and 220 reflections are given in Table 1. There are eight orientations of grains with a common [111] zone axis that are sampled to make up the observed pattern. The 211 reflections at 70.5° and the 220 reflections at 0° come from the two projections of the unit cell with the {111} planes parallel to the shear direction and the {220} planes along the shear gradient, i.e. perpendicular to the shear plates and the X-ray beam. The shear conditions used have obviously caused preferential orientation about this direction and this

is seen by the fact that these reflections are at least twice as strong as predicted (see Table 1). Furthermore the samples were cooled slowly after shear orientation so the [220] direction is also preferentially aligned along the thermal gradient during crystallisation. We conclude that the sample crystallises most rapidly along a [211] direction in grains which are oriented with their <220> directions parallel to the shear and thermal gradient. Furthermore grains with this orientation in the melt are observed to be in the Bragg conditions at least twice as frequently as in a randomly rotated set of grains. Crystallisation could select these grains to

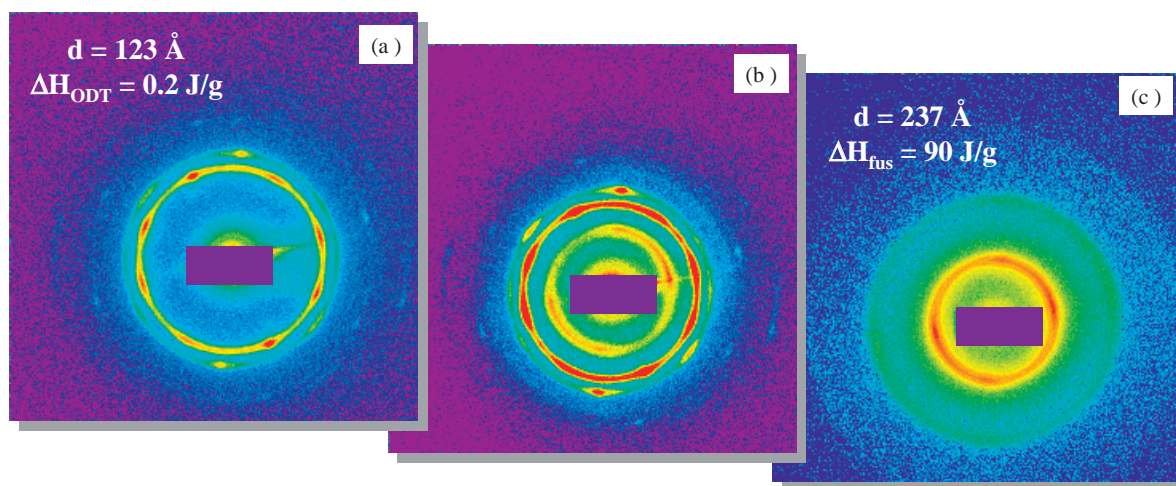


Figure 2: A series of SAXS patterns showing the transformation of a bicontinuous (Ia3d) cubic melt of $E_{75}B_{54}$ into an oriented lamellar crystal. (a) The (inner)10 spot pattern is from a 2D powder made up of grains rotated randomly around the [111] lattice direction which has become preferentially oriented parallel to the shear. (b) Once crystallisation starts strong scattering is observed inside the $\langle 211 \rangle$ reflections of the melt. Lamellar crystals, nucleated from the cubic melt, are observed to grow in a number of preferred directions, corresponding to the $\langle 211 \rangle$ and $\langle 220 \rangle$ reflections of the Ia3d. These lamellar crystals are consuming the ordered melt and the higher orders of the Ia3d are still clearly visible. (c) Eventually the Ia3d melt is nearly all consumed and higher order reflections can be seen for the lamellar crystals. There has been a transformation along the two crystallographic planes of the Ia3d cubic structure with d-spacing $123 \pm 2 \text{ \AA}$ to an oriented lamellar structure with d-spacing $237 \pm 5 \text{ \AA}$.

crystallise in the thermal gradient direction, consuming the other adjacent orientations. The SAXS patterns in Figure 4a indicate that the grains are of the order of $10 \mu\text{m}$ in size and only two orientations (and possibly tens of grains) are sampled in Figure 4a. In contrast there are many grains sampled in Figure 4b where there are oriented peaks on a strong lamellar ring.

Summary and Conclusions

We have demonstrated here that an interfacial preordering effect can cause crystallographic register to jump length scales in soft-hard templating. The retention of layer planes on crystallisation from an ordered melt is caused by the local stretching of chains and the locally one dimensional structure, despite the relative strengths of the structural process. What is unexpected, however, is that a complex soft structure will also direct the crystallisation processes, selecting specific orientations. We have considered many options for this, including low-angle grain boundaries, but conclude that there is a subtlety in the local chain orientation that provides the selection process. Small soft structures (lipid membranes) directing larger

hierarchical structures (bone and exoskeleton) are common in natural systems. We present here a soft matter system showing epitaxial crystallisation and length-scale jumping.

References

- [1] P. Ball, *The self-made tapestry*, Oxford University Press 1998
- [2] J.M. Seddon, *Biochim. Biophys. Acta.*, 1031, 1 (1990).
- [3] I.W. Hamley, *The Physics of Block Copolymers*, Oxford University Press 1998
- [4] F.S. Bates, G.H. Fredrickson, *Ann. Rev. Mat. Sci.*, 26, 501 (1996).
- [5] E.L. Thomas, R.L. Lascanec, *Philos.Trans.R. Soc. London A*, 348, 149 (1994).
- [6] S. Förster, A.K. Khandpur, J. Zhao, F.S. Bates, I.W. Hamley, A.J.Ryan, W. Bras. *Macromolecules*, 27, 6922 (1994).
- [7] E.L. Thomas, D.M. Anderson, C.S. Henke, D. Hoffman, *Nature*, 334, 598 (1988).
- [8] D.A. Hajduk, M.B.Kossuth, M.A. Hillmyer, F.S. Bates, *J Phys Chem B*, 102, 4269

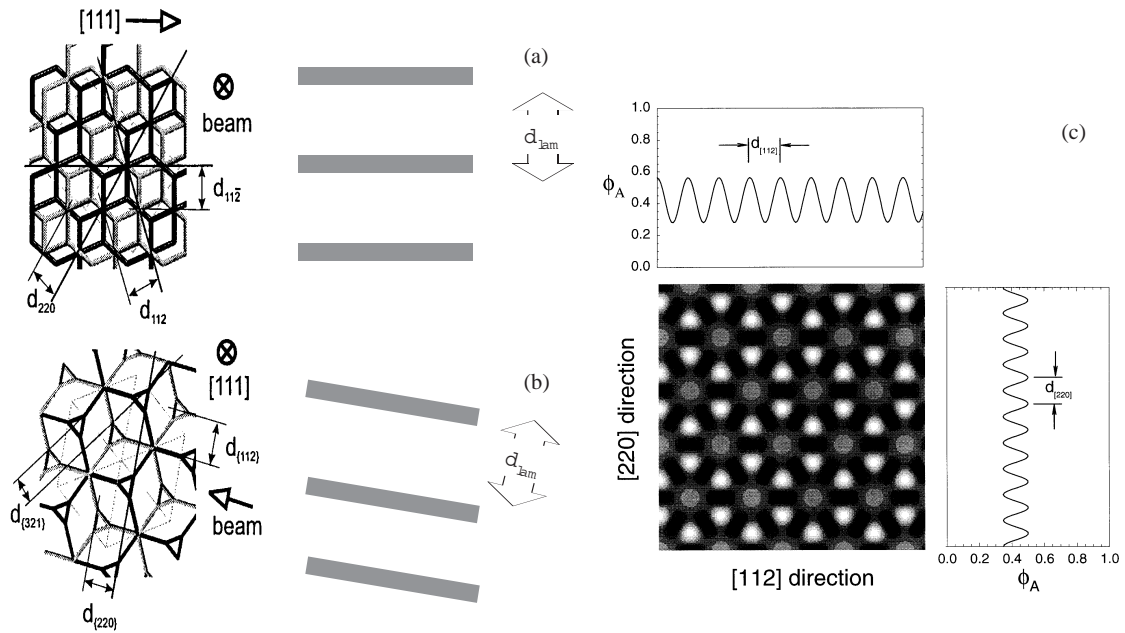


Figure 3: Schematics of the Ia3d morphology showing the orientation of the 3-functional connectors and the principal crystallographic directions. (a) A 2-dimensional projection [15] that shows the $\langle 112 \rangle$ and the $\langle 11\bar{2} \rangle$ reflections that are strongest in Figures 2a and 4a which transform into aligned lamellae by crystallisation along every second $\langle 11\bar{2} \rangle$ plane. (b) A view along the [111] direction [15] displaying $\{211\}$, $\{220\}$ and $\{321\}$ planes which transform into aligned lamellae by crystallisation along every second $\{211\}$ plane. (c) A 2-D image of composition, $\Phi_A(r)$, averaged in the [111] direction with the corresponding 1-D plots resulting from the average of $\Phi_A(r)$ in the [112] and [220] directions. This establishes that the gyroid phase is most lamellar-like in the [112] direction because the uppermost 1-D plot has the stronger oscillation.

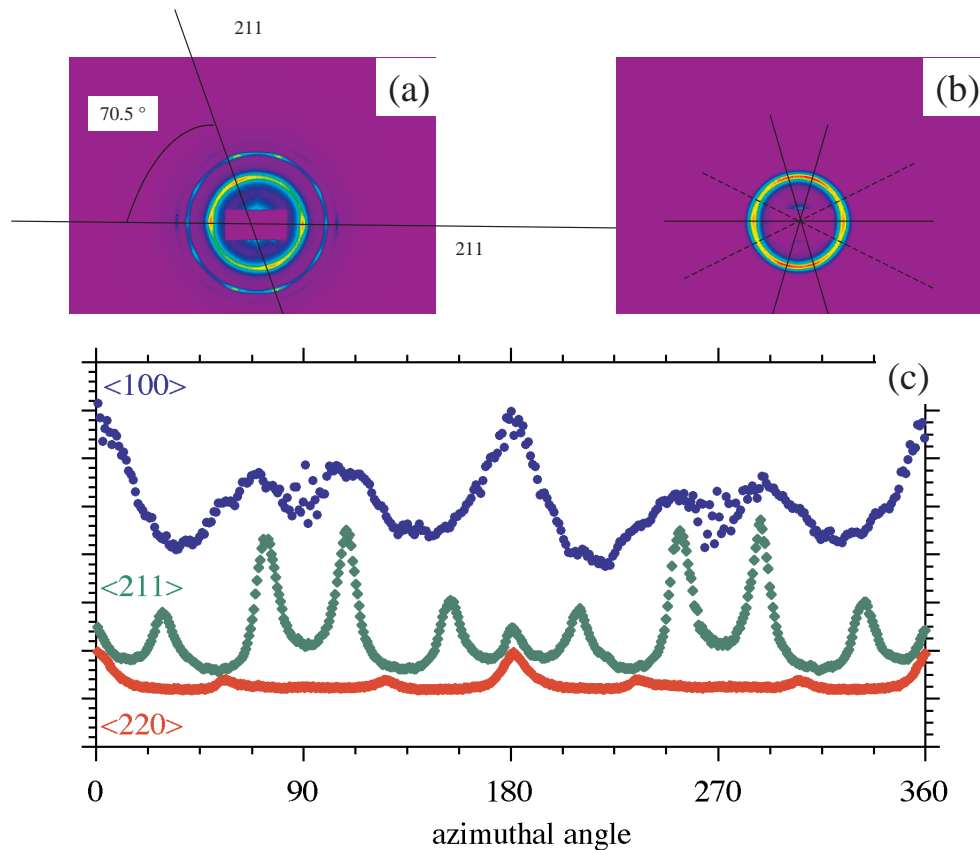


Figure 4; The relationship between the gyroid melt structure and the semicrystalline structure. (a) Superimposition of the SAXS patterns from the Ia3d melt and fully crystalline sample showing that the two lamellar orientations observed are consistent with the 112 and 11-2 reflections. The lamellar reflections are separated by 70.5° as expected for Ia3d [15]. The scattering measurements are made on a small scattering volume of 0.125 mm^3 and sample only a small number of grains. (b) Scattering from the same fully crystalline sample with a much larger scattering volume of 2.5 mm^3 . The solid lines show the $\langle 211 \rangle$ reflections that are followed by crystallisation, the dotted lines those not so obviously sampled. It should be noted that the peaks in the crystalline sample are superimposed on a bright ring implying some loss of overall orientation. (c) Azimuthal scans (with respect to the meridional direction) showing the relative intensities of the $\langle 211 \rangle$ and $\langle 220 \rangle$ in the melt compared to the crystalline lamellae $\langle 100 \rangle$ peaks in the solid.

- (1998).
- [9] M. Clerc, P. Laggner, A.-M. Levelut, G. Rapp, *J. Phys. France II*, 5, 901 (1995).
- [10] V. Luzzatti, *Nature*, 218, 1031 (1968).
- [11] M.W. Matsen, F.S. Bates, *Macromolecules*, 29, 1091 (1996).
- [12] D.A. Hajduk, P.E. Harper, S.M. Gruner, C.C. Honeker, G. Kim, E.L. Thomas, L.J. Fetters, *Macromolecule*, 27, 4063 (1994).
- [13] Y. Rancon, J. Charvolin, *J. Phys. Chem.*, 92, 2646 (1988).
- [14] P. Kekicheff, B. Cabane, *Acta. Crystallogr. B*, 44, 395 (1988).
- [15] M.E. Vigild, K. Almdal, K. Mortensen, I.W. Hamley, J.P.A. Fairclough, A.J. Ryan, *Macromolecules*, 31, 5702 (1998).
- [16] A. Firouzi, D. Kumar, L.M. Bull, T. Besier, P. Sieger, Q. Huo, S.A. Walker, J.A. Zasadzinski, C. Glinka, *Science*, 267, 1138 (1998).
- [17] D. Zhao et al, *Science*, 279, 548 (1998).
- [18] P.M. Lipic, F.S. Bates, M.A. Hillmyer, *J. Am. Chem. Soc.*, 120, 8963 (1998).
- [19] A. Kelarakis, W. Mingvanish, C. Daniel, H. Li, V. Havredaki, C. Booth, I.W. Hamley, A.J. Ryan, *Phys. Chem. Chem. Phys.* 2, 2755 (2000).
- 20 S.M. Mai, J.P.A. Fairclough, K. Viras, P.A. Gorry, I.W. Hamley, A.J. Ryan, C. Booth, *Macromolecules*, 30, 8392 (1997).
- 21 S-M. Mai, J.P.A. Fairclough, N.J. Terrill, S. Turner, I.W. Hamley, M.W.; Matsen, A.J. Ryan, C. Booth. *Macromolecules* 31, 8110- 8116, (1998).
- 22 Y Takahashi, H. Tadokoro, *Macromolecules*, 6, 672 (1973).
- 23 V.P. Voronov, V.M. Buleiko, V.E. Podneks, I.W. Hamley, J.P.A. Fairclough, A.J. Ryan, S-M Mai, B-X. Liao., *Macromolecules*, 30, 6674 (1997).
- 24 I.W. Hamley, J.P. Fairclough, N.J. Terrill, A.J. Ryan, P. Lipic, F.S. Bates, E. Towns-Andrews, *Macromolecules*, 29, 8835 (1996).
- 25 D.J. Quiram, R.A. Register, G.R. Marchand, D.H. Adamson, *Macromolecules*, 31, 4891 (1998).
- 26 M.W. Matsen, F.S. Bates, *Macromolecules*, 29, 7641(1996).
- 27 P.D. Olmsted, W.C.K. Poon, T.C.B. McLeish, N.J. Terrill and A.J. Ryan, *Phys. Rev. Lett.*, 81, .373 (1998).